Heregulin Reverses the Oligomerization of HER3[†]

Ralf Landgraf and David Eisenberg*

UCLA-DOE Laboratory of Structural Biology and Molecular Medicine, Molecular Biology Institute, Box 951570, Los Angeles, California 90095-1570

Received April 26, 2000

ABSTRACT: We analyzed the propensity of the HER3 receptor and its extracellular domain (ECD) to undergo ligand-independent self-association. The HER3-ECD, purified from *Drosophila* S2 cells, binds the EGF-like domain of heregulin (hrg) with a K_d of 1.9 nM as measured by surface plasmon resonance (SPR) studies. In a gel shift assay, the HER3-ECD self-associates into a uniform, slowly migrating species in a concentration-dependent manner, starting at concentrations of <10 nM. In contrast to the HER3-ECD, the ECD from the related HER2 receptor does not oligomerize under the same conditions. The direct interaction of HER3-ECDs was also demonstrated by pull-down assays and SPR measurements under physiological salt conditions. This self-association of the HER3-ECD was reversed by the addition of hrg but not by EGF. The apparent equilibrium dissociation constant for the HER3-ECD self-association is 15 nM, based on SPR measurements. In this analysis, hrg blocks HER3-ECD self-association, and the addition of hrg during the dissociation phase resulted in an accelerated off rate. This finding suggests that hrg can bind to and disrupt preexisting HER3-ECD oligomers. Full-length HER3 likewise exhibited self-association. Under conditions where co-immunoprecipitation and cross-linking of HER2 and HER3 were stimulated by hrg, HER3 self-association and cross-linking were disrupted by hrg. The implication is that the self-association of HER3-ECD favors the formation of catalytically inactive complexes of the HER3 receptor. Binding of hrg releases HER3 which may then form signaling-competent HER3−HER2 heterodimers.

HER3 (human epidermal growth factor receptor 3), also termed ErbB3, is a member of a family of type I receptor tyrosine kinases (*1*−*3*). The other members of this HER family are the EGF[1] receptor (EGFR), HER2, and HER4. The overexpression of HERs has been implicated in several solid tumor malignancies (*1*, *4*−*6*). HERs possess a cytoplasmic tyrosine kinase activity which is activated by the binding of peptide hormones such as EGF or heregulin and the subsequent formation of receptor dimers (*7*, *8*) or possibly higher-order complexes (*9*).

The amino acids of the four members of this receptor family are similar with a degree of identity of 36−48% in the extracellular domains, relative to EGFR, and 59−82% in their cytoplasmic kinase domains (*10*). However, the members of this family differ with respect to preferred ligands, affinity for their respective ligands (*11*), tyrosine kinase activity (*12*), and the rate of cellular downregulation (*13*). For example, HER2 possesses a potent tyrosine kinase activity but is unable to bind any of the known HER ligands by itself (*14*, *15*). HER3, on the other hand, has a relatively high affinity for heregulins (*15*, *16*), a family of EGF-like ligands also known as neuregulins, but is deficient in its tyrosine kinase activity (*12*). Therefore, it has to rely on the formation of mixed complexes with other HERs for effective signal transduction (*14*, *17*). In contrast, HER4 and EGFR are fully functional receptor kinases by themselves (*2*, *3*, *6*) but may also form heterodimers and thereby widen the spectrum of possible cellular responses (*10*, *18*, *19*).

In the case of HER2, overexpression results in ligand-independent tyrosine phosphorylation and cell proliferation (*20*, *21*). This concentration-dependent activation in the absence of ligand was also observed for recombinant HER2, purified in a baculovirus expression system, and correlated with the formation of an oligomeric receptor species (*22*). The extracellular domain of HER2 alone has been reported not to form such oligomers, and neither the ECD of HER2 nor HER3 can be induced to form oligomers by the addition of heregulin (*15*). As documented in this paper, we expressed both the extracellular domain of HER3 and the full-length receptor in *Drosophila* Schneider cells and observed a concentration-dependent self-association in the absence of heregulin. However, in contrast to EGFR, which can be induced to form dimers and oligomers with increased receptor or ligand concentrations (*23*), the HER3 complexes were disrupted by the addition of heregulin.

MATERIALS AND METHODS

Cloning and Expression of HER3 and HER2. The cDNA for HER3 was amplified from the total RNA of MCF7 cells (American Type Culture Collection, Rockville, MD) and HER2-transfected MCF7 cells (MCF7-HER2) (*21*) using the Advantage RT-PCR kit from Clonetech (Palo Alto, CA). Following amplification (N-terminal primer, C TCG GAG AGA TCT TCC GAG GTG GGC AAC TCT; C-terminal primer, C CAT GAC TCT AGA TGT CAG ATG GGT TTT

[†] We thank the National Institutes of Health for support.

* To whom correspondence should be addressed. Phone: (310) 825-3754. Fax: (310) 206-3914. E-mail: david@mbi.ucla.edu.

[1] Abbreviations: EGF, epidermal growth factor; hrg, EGF-like domain of heregulin; trx-hrg, thioredoxin fusion with hrg; rms, root-mean square; SPR, surface plasmon resonance; PBS, phosphate-buffered saline; ECD, extracellular domain.

10.1021/bi000953+ CCC: $19.00
Published on Web 06/27/2000

GC), the extracellular domain was cloned into the *Bgl*II and *Xba*I site of the pMT/BiP/V5-His A expression vector (Invitrogen, Carlsbad, CA). This vector features induction control through a metallothionin promotor and protein secretion using a *Drosophila* leader sequence. A C-terminal His tag and V5 epitope tag aid in purification and detection of the secreted ECDs. The transmembrane and cytoplasmic portions of HER3 were amplified by PCR and cloned into the sequence-confirmed ECD constructs, using the C-terminal *Xba*I site. Full-length HER2 was amplified and cloned into the *Sfi*I and *Xba*I site of pMT/BiP/V5-His A. The full-length receptors were designed to carry either a C-terminal V5 or myc tag but no His tag. All construct sequences were confirmed. S2 cells were cotransfected with the desired constructs and the pCoHYGRO vector (Invitrogen), which provides hygromycin resistance. A stable cell line was obtained after selection for 3 weeks with 300 μg/mL hygromycin (Invitrogen). For protein induction, 500 mL of cells in S2 medium (Sigma, St. Louis, MO) with 10% fetal bovine serum was grown to a cell density of approximately 6×10^6 cells/mL in a spinner flask and induced for 2 days at room temperature with 500 μM $CuSO_4$. Secreted proteins were precipitated with ammonium sulfate (80%), resolubilized, and purified on a 5 mL Pharmacia HITRAP Chelating column (Pharmacia, Picataway, NJ), loaded with $NiSO_4$. The protein eluted from the Hitrap column was found to be pure as judged by SDS−PAGE. The purified protein was dialyzed against PBS containing 1 mM EDTA followed by dialysis against PBS (150 mM NaCl, 2.5 mM KCl, 81 mM Na_2HPO_4, and 14.7 mM KH_2PO_4).

The ECD of HER2 was amplified as described above and cloned into the *Nco*I and *Xho*I site of the pMT/BiP/V5-His A expression vector. The expression and purification of this clone were carried out as described for HER3. A variant was generated for both ECDs which lacks the C-terminal V5 epitope, provided by the vector. For this purpose, an *Age*I restriction site was engineered at the C-terminus of both ECDs. Restriction digestion of the recipient vector with *Age*I removes the V5 epitope but maintains the His tag.

Expression and Purification of the EGF-like Domain of Heregulin. The 60-residue EGF-like domain of human heregulin β1 (residues 177−237) (hrg) was generated by a series of overlapping oligonucleotides and cloned into the *Eco*RI and *Hin*dIII site of the pET32-a expression vector (Novagen, Madison, WI) as described previously (*24*). The hrg domain was expressed in *Escherichia coli* BL21(DE3) cells as a thioredoxin fusion protein (trx-hrg) and was purified on a 5 mL Pharmacia HITRAP Chelating column, loaded with $NiSO_4$. The protein eluted from the Hitrap column was found to be >95% pure as judged by SDS−PAGE. The remaining impurity was predominantly free thioredoxin due to proteolysis. Prior to proteolytic cleavage of the fusion protein, trx-hrg was concentrated and dialyzed against 50 mM Tris (pH 8.0). $CaCl_2$ and Tween 20 were added to final concentrations of 10 mM and 0.1% (w/v), respectively. The proteolytic cleavage was carried out for 20 h at room temperature with 1 unit of enterokinase (Invitrogen) for every 3 mL of protein solution. The cleaved hrg domain was removed from residual uncleaved starting material by a second run on a Ni-chelating column. Residual enterokinase, detergent, and salts were removed by batch purification on a 20 cm^3 reversed phase column (Sep-Pak, Waters Corp., Milford, MA). For this purification, the protein was diluted 20-fold into aqueous 0.1% TFA and bound to the resin. After two washes with 20% acetonitrile and 0.1% TFA, hrg was eluted with 70% acetonitrile and 0.1% TFA and lyophilized. The final product was resolubilized and dialyzed against PBS.

Matrix-Assisted Laser Desorption Ionization (MALDI) Mass Spectrometry of HER3-ECD. HER3-ECD (0.9 mg/mL) in PBS was mixed on a gold-coated sample plate with 2.5 volumes of 10 mg/mL sinapinic acid in 70% acetonitrile and 0.1% trifluoroacetate. The sample was analyzed with a time-of-flight detector on a PerSeptive Biosystems Voyager RP mass spectrometer. The molecular mass was estimated from 128 averaged scans.

Gel Mobility Shift Assay for the Interaction of Hrg with the HER3-ECD. V5-tagged HER3-ECD (100 nM in PBS) was incubated (30 min at 4 °C) with recombinant hrg in PBS with 5% glycerol. Samples were run at 4 °C for 4 h with a 20 mA constant current on native 4 to 15% gradient gels (Bio-Rad, Hercules, CA) in 190 mM glycine and 25 mM Tris (pH 8.7). Following Western blotting, the HER3-ECD was visualized by chemiluminesence using a monoclonal antibody against the V5 epitope conjugated to horseradish peroxidase (HRP) (Invitrogen).

Self-Association of the HER-ECDs Assessesd by Gel Shift Analysis. HER2 (1 nM) or HER3-ECD (10 or 1 nM) carrying a C-terminal V5 tag (labeled ECD) was mixed with increasing concentrations of HER-ECD without the V5 tag (unlabeled ECD). Both proteins were incubated for 30 min at 4 °C in PBS and 5% glycerol. Samples were run on a 4 to 15% polyacrylamide gradient gel in a Tris/glycine buffer at 4 °C and visualized after Western blotting as described above.

Surface Plasmon Resonance Assessment of the HER3-ECD Interaction with the EGF-like Domain of Heregulin and Soluble HER3-ECD. For the assessment of hrg binding, the HER3-ECD (20 μg/mL) in MES buffer (100 mM, pH 6.0) was immobilized on a BIAcore CM5 chip using standard NHS/EDC amine coupling chemistry. The HER3-ECD was loaded on the chip by five consecutive loads until a final difference in response units (ΔRU) of 1500 was achieved. The residual ΔRU after fixation and blocking of the surface with ethanolamine was approximately 900 RU. The chip containing immobilized ECD could be regenerated through purging with 4 M NaCl and extensive washes with HEPES-buffered saline (HBS, Pharmacia). This high-salt wash disrupts HER3-ECD oligomerization and removes noncovalently bound ECDs from the chip. A thioredoxin fusion of the EGF-like domain of heregulin (trx-hrg) (*24*) in HBS was injected at various volumes and flow rates from 5 to 20 μL/min. Under these conditions, no mass transport effect was detected. For the determination of the dissociation constant, trx-hrg was applied to the chip at concentrations of 5, 10, 20, and 40 nM. All measurements were done in triplicate. The analysis of the data was done with the BIAcore software.

For measurements of the HER3-HER3 interaction, V5 antibodies were immobilized on a CM5 chip as described above (350 RU). A low load of V5-HER3-ECD (50 RU) was applied to the V5 antibody-loaded chip surface. Free ECD was removed through washes with 2 M NaCl and PBS (with 0.005% P20 surfactant, Pharmacia), and 200 nM HER3-ECD (no V5 tag) was applied to the chip in PBS (with

surfactant) at different flow rates ranging from 5 to 20 μL/min. Competition experiments with heregulin were carried out using only the EGF-like domain (hrg) of heregulin and were carried out in two different ways. For direct competition with HER3-ECD binding, hrg was added at equimolar concentrations (200 nM) to the running buffer (PBS and surfactant) and the HER3-ECD sample. To measure the effect of hrg on the off rate of the HER3-ECD, running buffer containing 20 nM hrg was injected during the dissociation stage of previously bound HER3-ECD (400 nM). All samples were filtered through 0.1 μm filter units (Millipore, Bedford, MA) just prior to the SPR measurements.

"Pull Down" of Soluble V5-HER3-ECD by Immobilized HER3-ECD. The HER3-ECD (no V5 tag) (1.5 mg) was coupled to 1 g of CNBr-activated Sepharose 4 (Pharmacia) using the coupling procedure recommended by the manufacturer. Using the same procedure, activated Sepharose was treated with 100 mM ethanolamine to provide deactivated resin for the negative control experiments. The coupled Sepharose (10 mL suspension) was washed with 4 M NaCl and PBS before use. For binding studies, the Sepharose resin (5 mL) was blocked with 1 mg/mL BSA in PBS for 15 min at room temperature. Following blocking, the V5-HER3-ECD was added to a final concentration of 200 nM. After 10 min at room temperature, the resin was washed in a column by gravity flow (5 $\times$ 50 mL of PBS). The resin was resuspended in 5 mL of PBS. Aliquots of 500 μL were transferred to 1.5 mL filter units (0.2 μm, Millipore) and drained by centrifugation at 200*g* for 3 min. The individual samples were resuspended in PBS containing different competing ligands, as indicated in Figure 4. After a 2 min incubation at room temperature, samples were spun again at 200*g* for 3 min, and the flow-through was analyzed by Western blot as described above.

Multiangle Static Light Scattering of the HER-ECD. Protein separation by size exclusion chromatography was achieved using a Superose 12 column (Pharmacia). The HER3-ECD was dialyzed into 50 mM Tris/acetate (pH 8.0) and was injected at a concentration of 1.44 mg/mL (20 μM) and a flow rate of 0.4 mL/min. The protein was detected at 214 nm, and the extinction coefficient for the HER3-ECD in Tris/acetate buffer at this wavelength was determined spectroscopically from samples with known concentrations. The refractive index increment (d*n*/d*c*) for the protein portion of the HER3-ECD in this buffer was assumed to be comparable to that of a monomeric BSA standard (Sigma). The carbohydrate content of 12% is expected to have a slightly lower d*n*/d*c* than the protein component. This proportional contribution of the carbohydrate component was modeled on the basis of known d*n*/d*c* values for different complex carbohydrates (*25*, *26*). The carbohydrate d*n*/d*c* contribution was estimated to be 0.157 and was integrated into the final d*n*/d*c* proportionally. The carbohydrate-corrected d*n*/d*c* was estimated to be 0.186. Molecular mass determination was carried out for those portions of the chromatogram which gave a sufficiently monodisperse scattering signal. Molecular mass estimates are the average of two independent runs. All measurements were carried out on a miniDAWN three-angle light scattering instrument (Wyatt Technology, Santa Barbara, CA), and data analysis was carried out using the accompanying ASTRA software.

Co-Immunoprecipitation and Cross-Linking of Full-Length HER3 and HER2. Stable, doubly transfected S2 cells, carrying full-length HER3(myc) and either HER3(V5) or HER2(V5), were induced with 500 μM $CuSO_4$, 48 h prior to the experiment. Cells were washed twice in PBS and resuspended at a concentration of 5×10^7 cells/mL. Aliquots of 100 μL were incubated at 4 °C for 15 min in the presence or absence of 5 nM hrg. Next, 2 μL of BS^3 bifunctional cross-linking reagent [bis(sulfosuccinimidyl) suberate, Pierce Biochemicals, Rockford, IL; dissolved in 5 mM sodium citrate (pH 5), final concentration of 200 μM] was added to selected samples. After 1 h at 4 °C, 10 μL of 1 M Tris (pH 8.0) was added to quench the cross-linking reaction. After 10 min, cells were spun at 1000*g* for 2 min and the cell pellet was lysed in mild lysis buffer [20 mM Tris (pH 8.0), 137 mM NaCl, 1% Triton X-100, 10% glycerol, 5 mM EDTA, 1 mM sodium orthovanadate, 1 mM phenylmethanesulfinyl fluoride, 1 μg/mL leupeptin, and 1 μg/mL aprotinin]. Insoluble material was cleared by centrifugation at 10000*g* for 10 min, and the resulting protein was quantitated using BCA (Pierce Biochemicals). Protein lysate (250 μg), mouse anti-myc antibody (2 μg, Invitrogen), and protein A/G agarose suspension (50 μL, Santa Cruz Biotechnology, Santa Cruz, CA) were incubated with gentle agitation for 12 h at 4 °C. After three washes with 1 mL of lysis buffer, the agarose pellet was resuspended in 50 μL of SDS−PAGE sample buffer. Samples (20 μL) of each reaction mixture were analyzed by SDS−PAGE, Western blotting, and probing with HRP-conjugated anti-V5 antibodies as described above.

RESULTS

Analysis of the Recombinant HER3-ECD. The recombinant HER3-ECD generated in *Drosophila* S2 cells was analyzed by SDS−PAGE to evaluate the purity and by mass spectrometry to estimate the carbohydrate content. The molecular mass of the ECD, as determined by MALDI mass spectrometry, is 82 kDa compared to a theoretical molecular mass for the protein component of 72 kDa (69 kDa without the six-His tag and V5 epitope). This difference is consistent with a carbohydrate content of 12% (16% with respect to the ECD without the His and V5 tags) and is in good agreement with ECDs expressed in Chinese hamster ovary (CHO) cells [published molecular mass of 80−84 kDa, 15−19% carbohydrate content (*15*)].

Binding of the EGF-like domain (hrg) of heregulin to the HER3-ECD was analyzed by plasmon surface resonance (SPR, BIAcore) measurements. For these measurements, we immobilized the HER3-ECD and varied the concentration of a thrioredoxin−hrg fusion protein. Changes in surface plasmon resonance are directly linked to the size of the particle brought into the proximity of the surface of the observation chamber. Fusion proteins of thioredoxin and hrg are approximately 4 times the size of hrg and are known to have binding properties comparable to those of the free hrg domain (*27*). The association and dissociation kinetics of trx-hrg are shown in Figure 1 for four different concentrations of trx-hrg. The equilibrium dissociation constant, calculated directly from k_{on} and k_{off}, is 1.9 nM [$k_{on} = (3.72 \pm 0.04) \times 10^6$ M^{-1} s^{-1}, $k_{off} = (7.3 \pm 1) \times 10^{-3}$ s^{-1}].

Gel Shift of the HER3-ECD by Hrg. The effect of heregulin binding to the HER3-ECD was also visualized by a gel

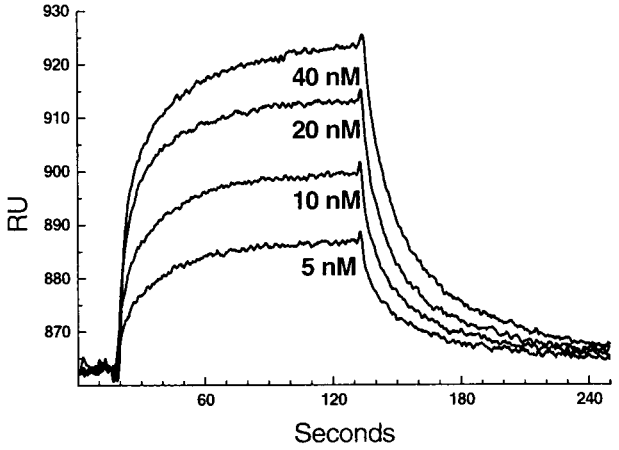

FIGURE 1: Sensorgram showing the binding of a thioredoxin-hrg fusion protein (trx-hrg) to the immobilized HER3-ECD. The *Y*-axis shows the time-dependent change in response units (RU) obtained with four different concentrations of thioredoxin-hrg. Starting with the smallest signal, the concentrations were 5, 10, 20, and 40 nM trx-hrg. The average of three independent sets of data indicates an equilibrium dissociation constant of 1.9 nM. Thus, hrg binding to the HER3-ECD from *Drosophila* S2 cells is comparable to that of HER3-ECDs from mammalian sources.

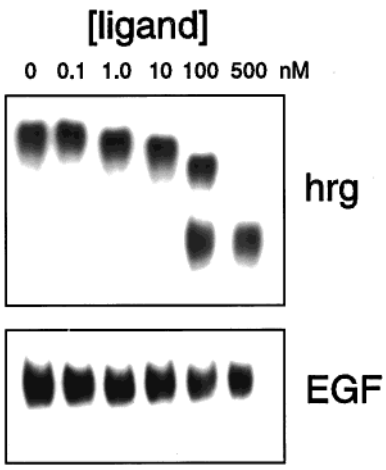

FIGURE 2: Shift in the electrophoretic mobility of the HER3-ECD upon addition of the EGF-like domain (hrg) of heregulin which suggests oligomeric HER3-ECD in the absence of ligand. Increasing concentrations of hrg or EGF (indicated in nanomolar above each lane) were added to V5-tagged HER3-ECD (100 nM). The HER3-ECD was detected with HRP-conjugated anti-V5 antibodies. An increase in the electrophoretic mobility of the HER3-ECD occurs through several intermediates upon addition of hrg but not EGF.

mobility shift assay (Figure 2). A constant concentration of 100 nM V5-tagged HER3-ECD (V5-HER3-ECD) was exposed to different concentrations of hrg, ranging from substoichiometric to excess concentrations. Upon addition of hrg, the HER3-ECD exhibited increased electrophoretic mobility. A minor shift could be observed at substoichiometric concentrations of hrg, and increased shifts occurred at higher hrg concentrations. This shift occurred through several intermediate stages of enhanced increases in mobility. Over the same concentration range, EGF failed to elicit a change in electrophoretic mobility.

Concentration-Dependent Self-Association of the HER3-ECD. The HER3-ECD has been reported to bind hrg with a 1:1 stoichiometry (*15*). The downward shift of the HER3-ECD upon addition of hrg and the presence of intermediates (Figure 2) prompted us to investigate the possibility that the

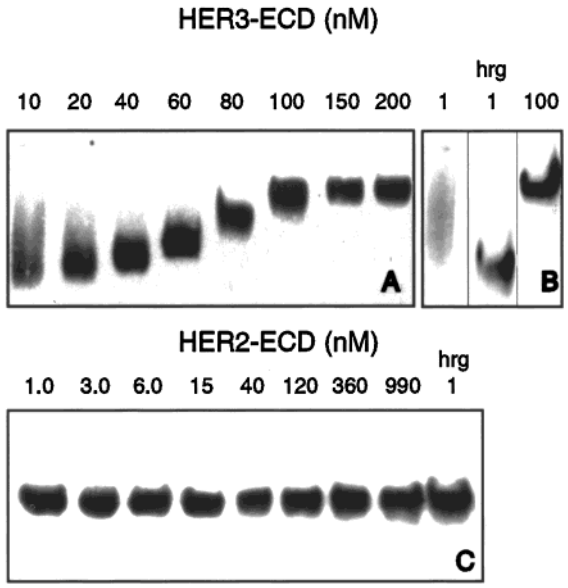

FIGURE 3: The ECD of HER3, but not HER2, self-associates in a concentration-dependent manner. Total concentrations (tagged and untagged) for each ECD are indicated in nanomolar above each lane. The addition of 5 nM hrg is indicated as "hrg". (A) Gel mobility shift assay of the HER3-ECD self-association. Increasing concentrations of untagged HER3-ECD were added to a constant concentration (10 nM) of V5-HER3-ECD. Increasing concentrations of the ECD resulted in more focused bands of decreasing electrophoretic mobility. No change in electrophoretic mobility occurred above 100 nM total ECD. (B) A low (1 nM) concentration of tagged HER3-ECD resulted in a diffuse and barely detectable band. Addition of (5 nM) hrg or untagged HER3-ECD (final concentration of 200 nM) resulted in the convergence of the tagged ECD into a single band. (C) The homologous ECD of HER2 (1 nM constant tagged ECD) showed no change in electrophoretic mobility with increases of the ECD concentration or addition of a 5-fold excess of hrg.

unshifted parent band represented an oligomeric species of the ECD. To this end, we analyzed the electrophoretic mobility of the ECD as a function of the total HER3-ECD concentration. A constant concentration of the HER3-ECD with a V5 epitope tag (10 nM) was incubated with increasing concentrations of non-V5 tagged ECD (Figure 3A). The change in mobility of the V5-tagged species was evaluated following Western blotting with anti-V5 antibodies. Two features stand out in this analysis. First, at 10 nM, the HER3-ECD failed to run as a discrete band. Second, the position of the HER3-ECD band shifted to progressively slower moving species, suggesting a self-association of the protein. The detection system used for this assay requires a minimum of 10 nM V5-HER3-ECD to permit a uniform exposure over the entire range of the gradient. When a low concentration of the V5-HER3-ECD (1 nM) was used, the V5-tagged ECD was easily detectable when consolidated into a single band through addition of hrg or high total HER3 concentrations (Figure 3B). ECD at 1 nM alone resulted in a diffuse band at the detection limit of the assay and was consequently underrepresented on Western blots. In a control reaction with the homologous ECD of HER2 (Figure 3C), no change in mobility is observed as the concentration of the ECD is increased or hrg is added.

To confirm that the changes in electrophoretic mobility upon addition of hrg were the result of the disruption of HER3-HER3 interactions, we used a pull down assay under physiological salt conditions. In this analysis, we measured

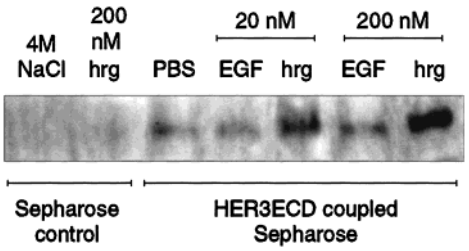

FIGURE 4: Soluble V5-HER3-ECD binds to immobilized HER3-ECD and can be specifically eluted with hrg. Soluble V5-HER3-ECD (200 nM) was added to Sepharose coupled with HER3-ECD (right) or control resin blocked with ethanolamine (left). Following washes, the resin was treated with the ligands indicated on top of each lane at the indicated concentrations. The eluate was analyzed by Western blotting using HRP-conjugated anti-V5 antibodies. Elution of the V5-HER3-ECD was dependent on immobilized HER3-ECD, and elution was most efficient with hrg. EGF, at high concentrations, was only marginally more effective than unchallenged dissociation in PBS.

the amount of V5-HER3-ECD that dissociated from immobilized HER3-ECD by addition of hrg. Following extensive blocking and washing steps, V5-tagged HER3-ECD remained bound to the HER3-ECD Sepharose resin (Figure 4). In a control experiment, neither specific elution with hrg nor a wash with 4 M NaCl released any soluble V5-HER3-ECD from Sepharose, which lacks immobilized HER3-ECD. Using the HER3-ECD-coupled Sepharose, soluble ECD could be eluted with hrg in a concentration-dependent manner. In contrast, EGF was not effective in dissociating the V5-HER3-ECD from the immobilzed ECD. At 20 nM ligand, significant amounts of ECD were released by hrg, but no enhanced dissociation could be observed with EGF. The amount of V5-tagged HER3-ECD, eluted with 200 nM EGF, was only marginally above the control for the unchallenged dissociation in PBS.

The diffuse nature of the ECD bands at low concentrations and the gradual dissociation of the HER3 in the pull down assay (Figure 4, PBS lane) limit quantitative measurements of the ECD interaction with those assays. To obtain an estimate of the underlying binding, we immobilized small amounts of the V5-HER3-ECD (50 RU) on a V5 antibody-coated BIAcore chip via the C-terminal V5 epitope tag of the ECD (Figure 5A). SPR measurements using (non V5-tagged) HER3-ECD showed binding to the immobilized ECD with a calculated equilibrium dissociation constant of 15 nM [$k_{on} = (18.3 \pm 3.2) \times 10^4\ M^{-1}\ s^{-1}$, $k_{off} = (28 \pm 14) \times 10^{-4}\ s^{-1}$]. This interaction could be inhibited by stoichiometric concentrations of hrg in the running buffer (Figure 5A). Moreover, addition of hrg during the dissociation phase of the HER3-ECD enhanced the dissociation rate (Figure 5B). The EGF-like domain (hrg) of heregulin was chosen for this analysis as opposed to the trx-hrg fusion protein used to establish the binding constant for the HER3-hrg interaction. The small size (6.6 kDa) of the hrg domain, relative to the soluble HER3-ECD (82 kDa), and the low HER3-ECD(V5) occupancy of the chip (50 RU) ensure that the binding of hrg does not result in a significant positive SPR signal by itself.

To investigate further the nature of the high-molecular mass species formed at concentrations of ECD greater than 100 nM, we used size exclusion chromatography and multiangle static light scattering. The in-line measurement

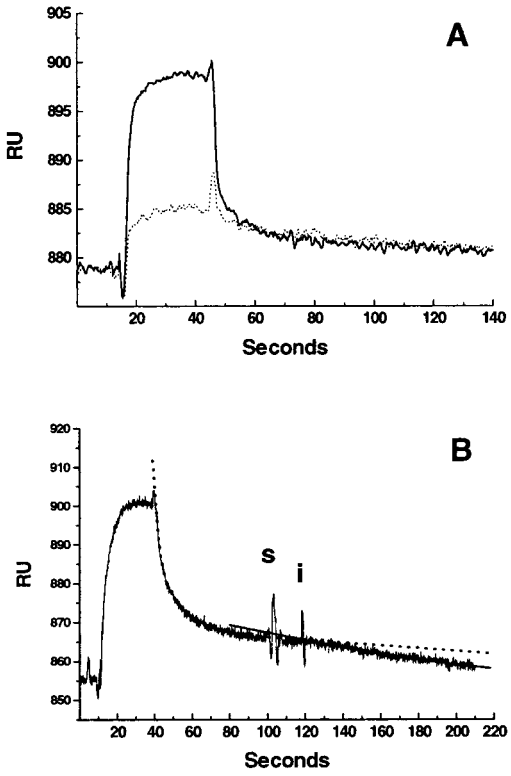

FIGURE 5: Sensorgram showing the binding of the HER3-ECD to the immobilized V5-HER3-ECD. Amine-coupled anti-V5 antibodies were loaded with small amounts (50 RU) of the V5-HER3-ECD. HER3-ECD was applied at a rate of 10 μL/min. (A) The binding of 200 nM (untagged) HER3-ECD (solid line) can be inhibited by the addition of equimolar hrg in the running buffer (dotted line). The sensorgram of the hrg-inhibited binding was superimposed on the basis of its baseline prior to the injection of the HER3-ECD. (B) The dissociation of the HER3-ECD (400 nM) is enhanced by 20 nM hrg. At the time point marked "s", the washing step of the HER3-ECD injection was stopped, and running buffer containing 20 nM hrg was injected instead at time point "i". The curve fit for an exponential signal decay is indicated in the absence (dashed line) and presence (solid line) of hrg. At the low V5-HER3-ECD occupancy of the chip and the small size of the 60-amino acid hrg domain, no significant positive signal results from the hrg injection alone (data not shown).

of multiangle static light scattering makes it possible to determine the molecular mass of the protein, independent of its elution time. The only requirements are that the light scattering from proteins, separated by chromatography, is monodisperse and that the refractive index increment (dn/dc) of the buffer used for the analysis has been determined by comparison with a known protein standard.

The outcome of this analysis is shown in Figure 6. As a result of dilution during the size exclusion chromatography, the concentration of the HER3-ECD at the time of light scattering ranged from 100 to 200 nM for different peaks. At this concentration, a dominant high-molecular mass species was observed, followed by a series of lower-molecular mass intermediates (Figure 6A, dotted line). Upon addition of a 5-fold excess of hrg, the HER3-ECD showed a substantial shift toward a lower-molecular mass species (Figure 6A, solid line)

The analysis of the light scattering signal from these elution profiles indicated that the high-molecular mass peak (peak I) has an estimated molecular mass of 980 $\pm$ 20 kDa or 12 copies of the HER3-ECD (Figure 6B). Protein samples

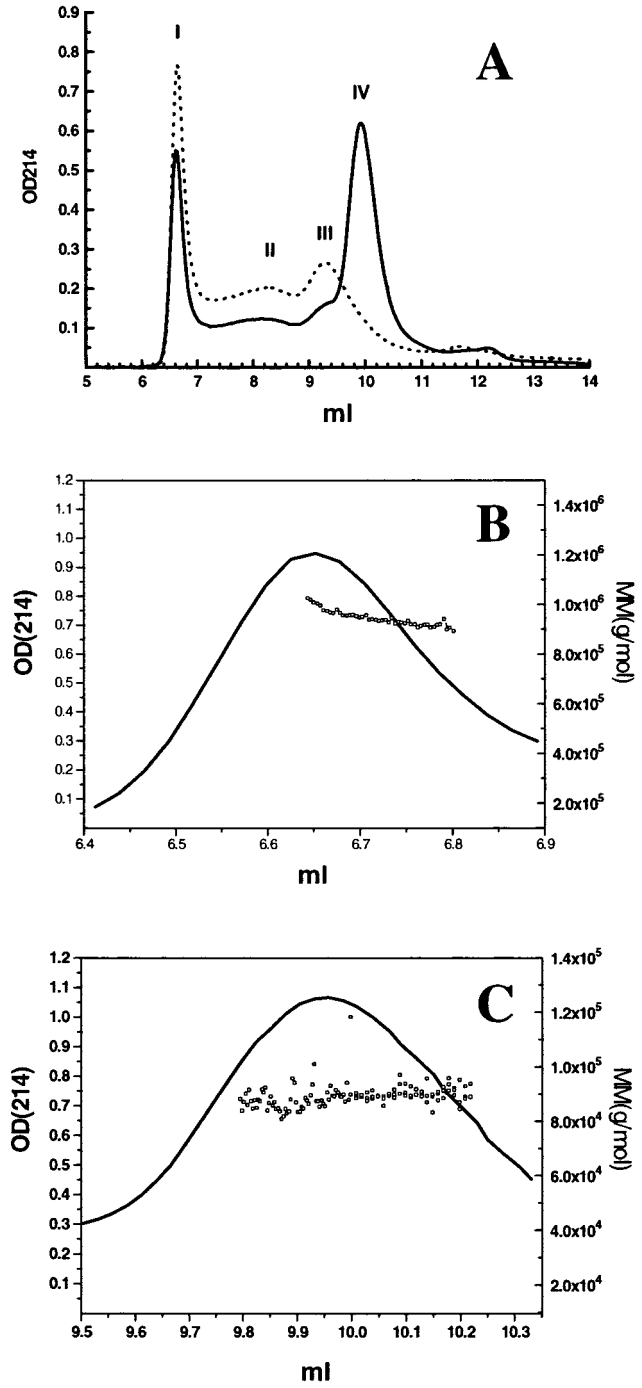

FIGURE 6: In the absence of hrg, a dodecamer represents the upper limit of HER3-ECD self-association. (A) Size exclusion chromatography of the HER3-ECD (dotted line) and the HER3-ECD, preincubated with a 5-fold excess of hrg (solid line). Binding of hrg to the HER3-ECD resulted in the decrease of the magnitude of the highest-molecular mass species (peak I) and a shift toward a low-molecular mass species (peak IV). (B) Multiangle light scattering analysis over peak I. The estimated molecular mass (squares) and the UV absorbance (solid line) are plotted against the elution volume, measured in milliliters. The light scattering analysis from the first section of the peak was not used to estimate the molecular mass due to overlapping scatter from a nonproteinacious, high-molecular mass impurity. The average molecular mass corresponds to 980 ± 20 kDa or 12 copies of the HER3-ECD. (C) Estimated molecular mass (squares) and UV absorbance (solid line) of peak IV. The average molecular mass of 89 ± 4 kDa corresponds best with a 1:1 complex of monomeric HER3-ECD and hrg.

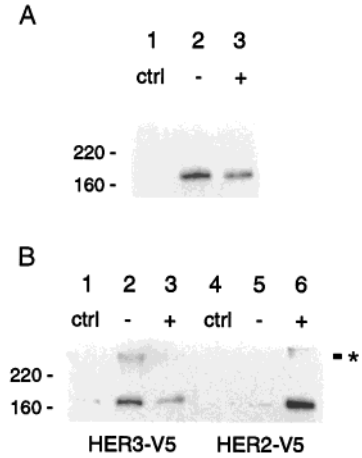

FIGURE 7: The self-association of full-length HER3 receptors is disrupted by hrg. (A) S2 cells containing HER3(myc) and HER3-(V5) were lysed, immunoprecipitated with anti myc antibody, and probed for the V5 epitope. The presence or absence of 5 nM hrg prior to lysis is indicated with + and −, respectively. The control reaction (lane 1 in panel A and lanes 1 and 4 in panel B) lacked anti myc antibody. The migration of molecular mass markers (in kilodaltons) is indicated to the left. This immunoprecipitation demonstrates HER3 self-association and its disruption by hrg. (B) Heregulin has opposite effects on HER3 oligomerization and HER3-HER2 association. S2 cells containing HER3(myc) and either HER3(V5) or HER2(V5) (as marked below) were treated with BS^3 cross-linking reagent prior to lysis. Cell lysates were analyzed as described for panel A. The location of co-immunoprecipitated and cross-linked products is indicated with an asterisk. The presence of cross-linked products demonstrates that the observed interactions occurred prior to cell lysis.

derived from cell culture supernatant contained a high-molecular mass impurity (>1500 kDa), which did not exhibit UV absorbance at 214 nm. The light scattering signal used for the molecular mass determination of the HER3-ECD was truncated to eliminate the contribution by this nonproteinacious impurity. The minor species observed in the absence of hrg (peaks II and III) have estimated molecular masses of 370 ± 30 and 200 ± 20 kDa. Due to the lower intensity of the scattering signal from these two species, a greater margin of error was associated with this measurement and the peaks correspond to 4.5. and 2.4 multiples, respectively, of the HER3-ECD molecular mass. The dominant peak generated by competition with hrg (peak IV) had an estimated molecular mass of 89 ± 4 kDa. This corresponds to the expected molecular mass for a monomeric HER3-ECD with hrg (82 and 7 kDa, respectively). However, due to the 5% error associated with this measurement, the molecular mass does not prove the presence of hrg nor its stoichiometry of binding to HER3.

Self-Association of Full-Length HER3. To evaluate if the observed self-association of the HER3-ECD represents a property of the intact receptor, we expressed the full-length receptor in *Drosophila* cells. We chose *Drosophila* S2 cells because they had produced functional HER3-ECD and are void of endogenous HER2 or HER3. Full-length HER2 was also generated to evaluate the heterodimerization properties of the *Drosophila*-expressed HER3.

First, we evaluated the ability of myc-tagged HER3 [HER3(myc)] to co-immunoprecipitate full-length V5-tagged HER3 [HER3(V5)] (Figure 7A). In the absence of hrg, a significant signal can be obtained for HER3(V5) (lane 2), relative to the control experiment (lane 1), which lacked anti-myc antibody. The magnitude of the HER3(V5) signal is decreased in the presence of hrg (lane 3). This finding is

consistent with the observed effect of hrg on HER3-ECD self-association. To confirm that the observed interaction occurred prior to cell lysis, we used the membrane impermeable cross-linker BS^3 and quenched the cross-linking reaction prior to the addition of lysis buffer (Figure 7B). Under those conditions, non-cross-linked and cross-linked HER3-V5 can be observed in the absence of hrg (lane 2). The addition of hrg reduces the magnitude of the signal obtained for both HER3(V5) species (lane 3). To confirm the specificity of this reaction as well as the functionality of the HER3 receptor, we carried out the inverse experiment in which we probed for HER2(V5) after immunoprecipitation of HER3-(myc) in S2 cells coexpressing HER3(myc) and HER2(V5) (lanes 4−6). Heregulin-dependent co-immunoprecipitation of HER2 and HER3 is a well-established assay for the detection of ligand-dependent formation of HER receptor heterodimers (*14*). Under those conditions, no cross-linked and trace levels of non-cross-linked HER2(V5) can be detected in the absence of hrg (lane 5). The addition of heregulin results in the efficient immunoprecipitation of both non-cross-linked and cross-linked HER2-V5 (lane 6).

DISCUSSION

Biological Activity of the HER3-ECD from Schneider Cells. The general paradigm for the activation of type I receptor kinases by their respective growth factor ligands involves ligand-induced receptor association. We analyzed the propensity of the extracellular domain of HER3 as well as the full-length receptor to undergo ligand-independent association as well as the impact of heregulin on the association state. The ECD used in these experiments was produced in *Drosophila* S2 Schneider cells and matches preparations from mammalian cells in composition and biological activity. We qualitatively demonstrate binding of the EGF-like domain (hrg) of heregulin by a gel mobility shift assay (Figure 2). The dissociation constant of 1.9 nM, as measured by surface plasmon resonance measurements (Figure 1), compares to 1.3 nM for the HER3-ECD expressed in CHO cells (*11*), determined also by surface plasmon resonance measurements. Other published dissociation constants are 2.3 and 26 nM determined by [^{125}I]hrg displacement measurements (*28*) and by sedimentation equilibrium analysis (*15*), respectively.

In contrast to previous binding studies by surface plasmon resonance, in which hrg was immobilized, we choose the inverse procedure in which the HER3-ECD is immobilized. This was done to eliminate ambiguities that might arise from different association states of the ECD if its concentration were varied between runs. The low level of coupling to the chip and the high-salt washes was intended to minimize the presence of HER3-ECD oligomers on the chip surface. Since binding of heregulin results in the dissociation of HER3-ECD oligomers (Figures 2 and 4−6), the presence of any residual oligomeric HER3-ECD on the chip would result in a slower on rate, because the process of binding would also include oligomer dissociation. Under those circumstances, the observed dissociation constant would be higher than would be expected in the absence of residual HER3-ECD oligomers. To increase the signal intensity in these measurements, we used a fusion protein consisting of thioredoxin and hrg to increase the mass of the analyte. Similar dissociation constants have been reported for binding of hrg and trx-hrg to K562 cells expressing full-length HER3 in the absence of other HER receptors. The dissociation constants for binding of hrg and trx-hrg to cellular HER3 were 1.2 and 5.2 nM, respectively (*27*). In summary, the ECD expressed in *Drosophila* cells is biologically active and has binding properties that are comparable to those of protein preparations from mammalian cell lines.

Self-Association of the HER3-ECD. Using four independent assay systems, we observed a propensity of the extracellular domain of HER3 to undergo self-association in the absence of ligands. Of those four assays, the SPR measurement of the HER3-ECD interaction and the pull down by immobilized HER3-ECD used PBS throughout the entire course of the measurement to simulate physiological salt conditions. The gel shift analysis was carried out on samples that were incubated in PBS and suggests that the ECD already exists in an equilibrium of different association states at 1 nM (Figure 3B). A gradient from 10 to 200 nM HER3-ECD resulted in a decrease in electrophoretic mobility with increasing concentrations of ECD. Several intermediates could be observed leading to a discrete end point. This slowly migrating band was distinct from aggregate in that it readily entered the gel matrix. The possibility that oligomerization was caused by the C-terminal His and V5 tag can be excluded on the basis of the heregulin-dependent dissociation and the control experiment with the HER2-ECD. The HER2-ECD carries the same C-terminal tags and failed to oligomerize. Oligomerization is therefore an intrinsic property of the HER3-ECD.

We proceeded to obtain size estimates of this high-molecular mass species by static light scattering following gel filtration. This analysis indicated a dominant species with a mass equivalent to approximately 12 copies of the ECD (Figure 6). Smaller intermediates corresponding to 2−4 copies could also be identified. In the absence of hrg, no significant peak with the molecular mass of the monomeric HER3-ECD was present. However, these results have to be interpreted with caution due to the low-ionic strength conditions used in this assay. Using buffers of higher ionic strength (up to 100 mM Na_2SO_4) also resulted in several higher-molecular mass products, but the resulting spread of the peaks did not permit an accurate molecular mass determination by static light scattering (data not shown). On the other hand, at high ionic strengths and in the absence of ligand, no homogeneous monomeric species could be obtained either. Although the upper limit of 12 copies of the HER3-ECD may not represent the physiologically relevant species, it is further evidence that the association of the HER3-ECD is unlikely to represent nonspecific random aggregation.

Kinetic measurements of the interaction between HER3-ECDs by surface plasmon resonance suggested an equilibrium dissociation constant of 15 nM. This value coincides with the range at which the diffuse signal in gel shift assays was consolidated into a single band, which was subsequently shifted upward. However, when this dissociation constant is being considered, it is important to realize that its calculation is based on a simple binding model of two interacting monomers. On the basis of the gel shift results, which do not show homogeneous monomers at the lowest concentrations and feature multiple intermediates at higher concentrations, this is likely to be an oversimplification.

Antagonistic Effect of Heregulin Binding on Self-Association. The analysis of the extracellular domains of all members of the EGFR and HER family has contributed significantly to our understanding of receptor-ligand interaction (*15*, *23*, *29*−*31*). In the case of the EGF receptor ECD, binding of EGF shifts the equilibrium toward an oligomeric state of the ECD (*29*). For the HER3-ECD, no such ligand-induced oligomerization has been observed (*15*). Previous data suggest that the HER3-ECD-heregulin complex has a 1:1 stoichiometry (*15*). Our data suggest that heregulin not only fails to sponsor the formation of higher-order complexes of the HER3-ECD but also breaks apart preexisting HER3-ECD oligomers. We observed this activity of heregulin in all four assays used to investigate HER3-ECD self-association. Heregulin could achieve this by two different mechanisms. Heregulin could bind only to monomeric HER3-ECDs, block their self-association, and shift the equilibrium of free and associated ECDs toward the free species. Alternatively, heregulin could bind to and disrupt preexisting ECD oligomers. Assays that involve incubation steps during which hrg could shift an oligomer−monomer equilibrium cannot differentiate between both options. However, some insight is provided by the SPR measurements. The addition of the hrg domain to the running buffer during the dissociation phase of HER3-ECD resulted in an accelerated off rate. Although the difficult timing of the experiment does not allow for the collection of sufficient data for a quantitative analysis, this result is consistent with direct binding and disruption of HER3-ECD oligomers by hrg. This disruption of HER3-ECD oligomers is specific to heregulin. The closely related EGF fails to cause downward gel shifts and is only marginally active at high concentrations in dissociating HER3-ECDs from their Sepharose-immobilized counterparts.

Self-Association of Full-Length HER3 Receptors. While measurements on the ECD of HER3 provide insight into the affinity of the HER3 self-association, its possible stoichiometry, and the mode of oligomer disruption by heregulin, a key question remains: do these findings apply to the full-length receptor? The co-immuoprecipitation and cross-linking experiments (Figure 7) confirm both self-association of HER3 and heregulin-dependent dissociation for the intact receptor. The BS^3 cross-linking reaction (Figure 7B) has a low efficiency (approximately 5%), and the majority of the co-immunoprecipitated HER3(V5) signal results from noncovalent HER3-HER3 interactions. Thus, the cross-linking experiment cannot determine the stoichiometry of the HER3 association. However, since BS^3 does not cross biological membranes (*32*) and cross-linking was quenched prior to cell lysis, any cross-linking observed under those conditions occurred prior to lysis, and is therefore reflective of interactions on the surface of intact S2 cells. The magnitudes of both the signals from the cross-linked and non-cross-linked HER3 decrease upon addition of heregulin. This finding is in agreement with the data observed for the HER3-ECD. While the ECDs of HER3 and HER2 fail to form heterodimers upon addition of hrg (*33*), the biologically relevant heterodimerization can be reproduced for the full-length receptors (lane 6, Figure 7B), thus demonstrating the functionality and specificity of the HER3 and HER2 receptors used in this study. The observed stimulation of HER2-HER3 association is the opposite of hrg's disruptive effect on the self-association of HER3.

Biological Relevance of HER3 Self-Association. The results for the intact HER3 receptor qualitatively confirm the interaction seen for the ECD. The studies on the ECD provide information about the affinity of the underlying interaction and insights into the mechanism by which heregulin disrupts the receptor complexes. On the basis of available information for the ECDs of EGFR and HER2, the HER3-ECD stands out in its high propensity for self-association. Less is known about HER4, the most recent addition to this family of receptors. The concentration range at which the observed self-association of the HER3-ECD occurs is remarkable. A significantly higher concentration of at least several micromolar is required before the extracellular domain of EGFR shows signs of ligand-independent self-association (*23*, *31*). In contrast, the HER3-ECD self-associated in the low nanomolar range. The constraint to two dimensions for the membrane-bound ECD significantly enhances its effective concentration on the cell surface. Levels of HER3 expression vary between different mammalian cell lines with many cells carrying 10^3-10^4 receptors, based on direct (*34*) or indirect measurements (*35*). On the basis of an estimate for the effective concentration of the EGF receptor in a two-dimensional space (*31*, *36*), 10^3-10^4 receptors per cell would correspond to a concentration of 100 nM to 1 μM in solution. This concentration is well above the range at which the HER3-ECD undergoes a self-association in our analysis.

On the basis of this estimate for the effective concentration of surface-bound HER3 receptors, it is perhaps not surprising that the full-length receptor shows the same self-association as the ECD (Figure 7). On the contrary, it is surprising that hrg can disrupt these oligomers of membrane-located oligomers. Closer analysis of its disruptive effect in Figure 7 shows, in fact, that hrg is less effective in disrupting the HER3-HER3 interaction than it is in stimulating HER3-HER2 heterodimer formation. This may be a reflection of the 3 order of magnitude tighter binding of hrg to HER3-HER2 heterodimers than to HER3 monomers (*14*). The level of HER3 monomers is a reflection of the competition between HER3-HER3 self-association and hrg binding. On the basis of our study and published data on the properties of the ECD, both binding events have similar affinities in the low nanomolar range. However, in the presence of HER2, even small amounts of dissociated HER3-hrg complexes are likely to be "trapped" in the significantly more stable HER3-hrg-HER2 complexes. This would remove the necessity for high concentrations of hrg to disrupt HER3 association in vivo. Therefore, these competing associations may serve a role in ensuring hrg-dependent signaling while minimizing ligand-independent association and activation of HER3 and HER2.

While ligand-induced dimerization or oligomerization is a widespread mechanism for receptor activation, ligand-independent and noncovalent self-association has been reported for several other receptors such as the erythropoietin (Epo) receptor (*37*) or natriuretic peptide (NAP) receptor (*38*, *39*). In those cases, ligand binding is thought to modulate the activity of preexisting receptor complexes. Recent studies on the Epo receptor (*37*, *40*) suggest that changes in the relative orientation of the extracellular domains upon ligand binding change the spacing of the cytoplasmic domains and thus achieve activation. In the case of HER3, the ligand

likewise may bind to a self-associated state of the receptor. However, in contrast to EpoR or NAP, the HER3 receptor is nonfunctional by itself, and the result of ligand binding is the disruption of HER3-HER3 interactions in favor of HER3-HER2 complexes, the most potent form of activated HER receptors.

In conclusion, we demonstrate that the ECD of HER3 has a strong propensity to undergo self-association at low nanomolar concentrations. It does so in a manner that is distinct from random aggregation. Moreover, heregulin, but not EGF, reverses this ligand-independent self-association. Self-association and its reversal by heregulin were also qualitatively confirmed for the full-length receptor. The effect of heregulin on receptor association is therefore the opposite for HER3-HER3 and HER3-HER2 complexes. Although our study demonstrates that the properties of the ECD are sufficient to explain the observed self-association of the full-length HER3 receptor, the transmembrane and cytoplasmic portions may further modulate the observed interaction in vivo. On the basis of this study, further work on full-length HER3 is needed to evaluate how HER3 self-association affects signal transduction by this family of receptors.

ACKNOWLEDGMENT

We thank Dr. Edward Marcotte for his help with MALDI mass spectrometry, Martin Phillips for help with BiaCore measurements, Dr. Daniel Anderson for his help with multiangle static light scattering, and Lori Eldrege for her help with cell culture experiments.

REFERENCES

1. Kraus, M. H., Issing, W., Miki, T., Popescu, N. C., and Aaronson, S. A. (1989) *Proc. Natl. Acad. Sci. U.S.A. 86*, 9193−7.
2. Ullrich, A., and Schlessinger, J. (1990) *Cell 61*, 203−12.
3. Plowman, G. D., Culouscou, J. M., Whitney, G. S., Green, J. M., Carlton, G. W., Foy, L., Neubauer, M. G., and Shoyab, M. (1993) *Proc. Natl. Acad. Sci. U.S.A. 90*, 1746−50.
4. Slamon, D. J., and Clark, G. M. (1988) *Science 240*, 1795−8.
5. Dougall, W. C., Qian, X., and Greene, M. I. (1993) *J. Cell Biochem. 53*, 61−73.
6. Plowman, G. D., Green, J. M., Culouscou, J. M., Carlton, G. W., Rothwell, V. M., and Buckley, S. (1993) *Nature 366*, 473−5.
7. Yarden, Y., and Schlessinger, J. (1987) *Biochemistry 26*, 1434−42.
8. Yarden, Y., and Schlessinger, J. (1987) *Biochemistry 26*, 1443−51.
9. Huang, G. C., Ouyang, X., and Epstein, R. J. (1998) *Biochem. J. 331*, 113−9.
10. Earp, H. S., Dawson, T. L., Li, X., and Yu, H. (1995) *Breast Cancer Res. Treat. 35*, 115−32.
11. Tzahar, E., Pinkas-Kramarski, R., Moyer, J. D., Klapper, L. N., Alroy, I., Levkowitz, G., Shelly, M., Henis, S., Eisenstein, M., Ratzkin, B. J., Sela, M., Andrews, G. C., and Yarden, Y. (1997) *EMBO J. 16*, 4938−50.
12. Guy, P. M., Platko, J. V., Cantley, L. C., Cerione, R. A., and Carraway, K. L. r. (1994) *Proc. Natl. Acad. Sci. U.S.A. 91*, 8132−6.
13. Baulida, J., Kraus, M. H., Alimandi, M., Di Fiore, P. P., and Carpenter, G. (1996) *J. Biol. Chem. 271*, 5251−7.
14. Sliwkowski, M. X., Schaefer, G., Akita, R. W., Lofgren, J. A., Fitzpatrick, V. D., Nuijens, A., Fendly, B. M., Cerione, R. A., Vandlen, R. L., and Carraway, K. L. r. (1994) *J. Biol. Chem. 269*, 14661−5.
15. Horan, T., Wen, J., Arakawa, T., Liu, N., Brankow, D., Hu, S., Ratzkin, B., and Philo, J. S. (1995) *J. Biol. Chem. 270*, 24604−8.
16. Carraway, K. L. r., Sliwkowski, M. X., Akita, R., Platko, J. V., Guy, P. M., Nuijens, A., Diamonti, A. J., Vandlen, R. L., Cantley, L. C., and Cerione, R. A. (1994) *J. Biol. Chem. 269*, 14303−6.
17. Alimandi, M., Romano, A., Curia, M. C., Muraro, R., Fedi, P., Aaronson, S. A., Di Fiore, P. P., and Kraus, M. H. (1995) *Oncogene 10*, 1813−21.
18. Karunagaran, D., Tzahar, E., Beerli, R. R., Chen, X., Graus-Porta, D., Ratzkin, B. J., Seger, R., Hynes, N. E., and Yarden, Y. (1996) *EMBO J. 15*, 254−64.
19. Qian, X., LeVea, C. M., Freeman, J. K., Dougall, W. C., and Greene, M. I. (1994) *Proc. Natl. Acad. Sci. U.S.A. 91*, 1500−4.
20. Slamon, D. J., Clark, G. M., Wong, S. G., Levin, W. J., Ullrich, A., and McGuire, W. L. (1987) *Science 235*, 177−82.
21. Pegram, M. D., Finn, R. S., Arzoo, K., Beryt, M., Pietras, R. J., and Slamon, D. J. (1997) *Oncogene 15*, 537−47.
22. Samanta, A., LeVea, C. M., Dougall, W. C., Qian, X., and Greene, M. I. (1994) *Proc. Natl. Acad. Sci. U.S.A. 91*, 1711−5.
23. Hurwitz, D. R., Emanuel, S. L., Nathan, M. H., Sarver, N., Ullrich, A., Felder, S., Lax, I., and Schlessinger, J. (1991) *J. Biol. Chem. 266*, 22035−43.
24. Landgraf, R., Pegram, M. D., Slamon, D. J., and Eisenberg, D. S. (1998) *Biochemistry 37*, 3220−8.
25. Arakawa, T., Langley, K. E., Kameyama, K., and Takagi, T. (1992) *Anal. Biochem. 203*, 53−7.
26. Mueller, A., Pretus, H. A., McNamee, R. B., Jones, E. L., Browder, I. W., and Williams, D. L. (1995) *J. Chromatogr., B: Biomed. Sci. Appl. 666*, 283−90.
27. Jones, J. T., Ballinger, M. D., Pisacane, P. I., Lofgren, J. A., Fitzpatrick, V. D., Fairbrother, W. J., Wells, J. A., and Sliwkowski, M. X. (1998) *J. Biol. Chem. 273*, 11667−74.
28. Ballinger, M. D., Jones, J. T., Lofgren, J. A., Fairbrother, W. J., Akita, R. W., Sliwkowski, M. X., and Wells, J. A. (1998) *J. Biol. Chem. 273*, 11675−84.
29. Lax, I., Mitra, A. K., Ravera, C., Hurwitz, D. R., Rubinstein, M., Ullrich, A., Stroud, R. M., and Schlessinger, J. (1991) *J. Biol. Chem. 266*, 13828−33.
30. Zhou, M., Felder, S., Rubinstein, M., Hurwitz, D. R., Ullrich, A., Lax, I., and Schlessinger, J. (1993) *Biochemistry 32*, 8193−8.
31. Lemmon, M. A., Bu, Z., Ladbury, J. E., Zhou, M., Pinchasi, D., Lax, I., Engelman, D. M., and Schlessinger, J. (1997) *EMBO J. 16*, 281−94.
32. Knoller, S., Shpungin, S., and Pick, E. (1991) *J. Biol. Chem. 266*, 2795−804.
33. Fitzpatrick, V. D., Pisacane, P. I., Vandlen, R. L., and Sliwkowski, M. X. (1998) *FEBS Lett. 431*, 102−6.
34. Aguilar, Z., Akita, R. W., Finn, R. S., Ramos, B. L., Pegram, M. D., Kabbinavar, F. F., Pietras, R. J., Pisacane, P., Sliwkowski, M. X., and Slamon, D. J. (1999) *Oncogene 18*, 6050−62.
35. Lewis, G. D., Lofgren, J. A., McMurtrey, A. E., Nuijens, A., Fendly, B. M., Bauer, K. D., and Sliwkowski, M. X. (1996) *Cancer Res. 56*, 1457−65.
36. Schlessinger, J. (1979) *Receptor aggregation as a mechanism for transmembrane signalling: Models for hormone action*, Elsevier, Amsterdam.
37. Remy, I., Wilson, I. A., and Michnick, S. W. (1999) *Science 283*, 990−3.
38. Chinkers, M., and Wilson, E. M. (1992) *J. Biol. Chem. 267*, 18589−97.
39. Rondeau, J. J., McNicoll, N., Gagnon, J., Bouchard, N., Ong, H., and De Lean, A. (1995) *Biochemistry 34*, 2130−6.
40. Livnah, O., Stura, E. A., Middleton, S. A., Johnson, D. L., Jolliffe, L. K., and Wilson, I. A. (1999) *Science 283*, 987−90.

BI000953+